10.2514/6.2023-0997

# Detached Eddy Simulation of Unsteady Flow over a Frontal Cavity

Samruddhi Salunke[1] and Suryapratap Shinde[2] and Ishika Singh[3] and Devabrata Sahoo[4]
*MIT School of Engineering, MIT-Art Design and Technology University, Pune, India - 412201*

Ashish Vashishtha[5]
*South East Technological University, Carlow Campus, Ireland R93 V960*

**Frontal cavity consists of complex unsteadiness which causes bow shock instabilities when the body is moving at supersonic or hypersonic speed through a fluid. These complex unsteady flow fields are an important practical concern in the aerospace applications. Understanding this flow field around the frontal cavity will help us to know more in depth about these instabilities to create effective control methods to avoid structural damages. The main objective of the present research is to analyze the bow shock instabilities at different Mach number around the frontal cavity at supersonic and hypersonic speeds by using the numerical concept of Detached Eddy Simulations (DES) in two dimensional axisymmetric domain. Three different freestream Mach numbers (2, 4 and 6) were considered in the present investigation in order to study the effect of Mach number on flow unsteadiness. It was observed that an increase in Mach number, the frequency of most dominant mode (bow shock pulsation) increases significantly. In addition to that, additional low amplitude sub-dominant modes were observed for all the cases of freestream Mach numbers studied in the present investigation.**



## Nomenclature

$D$ = model diameter
$t$ = shell thickness
$M$ = freestream Mach number
$P_0$ = stagnation pressure
$T_0$ = stagnation temperature
$R_e$ = freestream Reynolds number

## I. Introduction

In general, it is noted that parachute slows the descent in the vertical direction of the falling body through the atmosphere and more particularly the parachutes have been used as an effective aerodynamic (supersonic / hypersonic) decelerator into low-density atmosphere for descent and recovery of aerospace vehicles in terrestrial and planetary missions. Therefore, simulation of parachute inflation through computational method has attracted attention of the researchers [1]. On that context, parachute-based decelerators have been tested as a supersonic or hypersonic inflated decelerators for mars space exploration [2]. Basically, aerodynamic decelerators play a key role in the entry, decent and landing of planetary exploration vehicles. Although effective decelerators seem to imply but limited to functioning as deceleration (often from supersonic to subsonic speeds) and terminal descent velocity control devices, it serves multiple purposes which is clear for engineers while designing, developing and qualifying the parachutes. These supersonic-based parachute decelerators have their applications included in aircraft extraction, supplementary braking in the aircrafts, braking race boats and emergency landing [1]. To avoid unsteadiness due to flexible surface of parachute

[1]Engineering Student, Department of Aerospace Engineering, MITSOE, MIT ADT University, Pune, INDIA
[2]Engineering Student, Department of Aerospace Engineering, MITSOE, MIT ADT University, Pune, INDIA
[3]Engineering Student, Department of Aerospace Engineering, MITSOE, MIT ADT University, Pune, INDIA
[4]Associate Professor, Department of Aerospace Engineering, MITSOE, MIT ADT University, Pune, INDIA
[5] Lecturer, Department of Aerospace & Mechanical Engineering, SETU, Carlow Campus, IRELAND and AIAA Senior Member

during wind tunnel experiments, rigid body with frontal cavity had been tested in many wind tunnel studies at supersonic and hypersonic speeds. Hatanaka et al. [3] identified the range of conditions, they would be expected to operate in, and suggested system configurations. Also, the use of such supersonic based parachutes has certain limitations, such as the unsteadiness observed around and ahead of the frontal cavity on the parachute deployment is the primary drawback which includes the aerodynamic interactions between the canopy shock and capsule [1, 3]. The Mach number, Reynolds number, size ratio of the canopy to the capsule, proximity, angle of attacks of the canopy and capsule and the material properties of the canopy are the basics criteria on which the wake depends upon [1, 3]. The uses of parachutes make them act as a means of effective decelerators because landing on mars is not like landing on earth, Mars has a tricky environment somewhere in between [4]. In addition, parachutes for mars surface-bound craft must be enormous because the atmosphere is too thin to fill a parachute like used on earth, powerful airbags have been definitely required to complete the landing. The second drawback arise during the deployment of parachutes which develops wrinkles and thereby make it difficult to study its aerodynamic characteristics [4]. Earlier, the wind tunnel investigations using the rigid shapes of developing aerodynamic decelerators for its application, the drag and stability at supersonic speeds of parachutes has been reported [3]. Also, the flow-field around a supersonic parachute along with the effects of suspension lines had also been studied [2]. The challenges such as accurate aerodynamics calculations for bluff-body geometries attracts the attention of researchers, and considerable achievements have been obtained in applying experimental methods [5–7] to different frontal cavity and its control [8]. However, capturing of large amplitude fluctuations using numerical simulations has been a challenging task because of the involvement of range of spatial and temporal scales in supersonic [3] and hypersonic flow [9]. These simulations (3-D frontal hemispherical cavity) do not employ any turbulence modelling. Also, high computational resources are required for above 3-D simulations. There are limitation with the laminar solver as they fail and become unstable due to rapid movement of frontal shocks [3, 9]. Later Jayraj et al. [10] reported that by the use of DES solver [11] the unsteadiness generating over the frontal cavity at supersonic speed of Mach 4.00 can be captured without the solution becoming unstable. In their study, they captured the complete unsteady pulsation cycle generating over a frontal cavity and explained the flow phenomena arising at a free stream Mach number of 4.00. As per [10], a simpler approach to capture the unsteadiness over frontal cavities at supersonic flow of Mach 4.00 has been provided, however the effect of free-stream Mach number on the unsteadiness over a frontal cavity is yet to be reported. This provided the motivation for the present research work. Based on the motivation gained, the objective of the present investigation is to computationally investigate the effect of free-stream Mach number on the flow unsteadiness arising in front of a frontal cavity. The objective is planned to be achieved by suitably computing the unsteadiness generated in front of the rigid hemispherical shells at two supersonic speeds (Mach 2.00 and Mach 4.00) as well as at one hypersonic speed of Mach 6.00. In order to study the effect of the Mach number on the flow unsteadiness, both qualitative and quantitative approach has been adopted. Time resolved Mach contours captured at different flow times are compared for different cases for analyzing the unsteadiness qualitative and pressure histories at various locations on and around the frontal cavity are captured in order to quantitatively analyze the effect of the free stream Mach number on the frequency and amplitude of the unsteadiness generated ahead of the frontal cavity.



## II. Computational Methodology

### A. Geometrical Details

The frontal cavity investigated in the present study is hemispherical in shape with the concave cavity facing the incoming high-speed flow. The geometrical specifications of the hemispherical cavity are similar to that adopted in Hatanaka et al [3]. The frontal cavity is hemispherical in shape with an internal diameter of 80 mm. The cavity has a shell thickness of 2.1 mm. The 2D hemispherical concave shell with the detailed geometrical specifications is presented in Fig. 1a. The experimental model is also connected with a 30 mm diameter sting at the base to connect in wind tunnel test-section, which is not considered in numerical simulation.

### B. Numerical Procedure

In the present paper, the 2D axisymmetric computations have been conducted at a freestream Mach number of 2.0, 4.0 and 6.0 using Detached Eddy Simulations (DES) with a commercial solver (Ansys-Fluent), to resolve the unsteady flow field observed over the frontal cavity geometry. The simulations have been performed by considering air as ideal gas. A coupled density-based solver with compressibility effects incorporated in the k-$\omega$ SST turbulence model has been adopted and the domain is discretized using the second order schemes both spatially and temporally. Detached Eddy

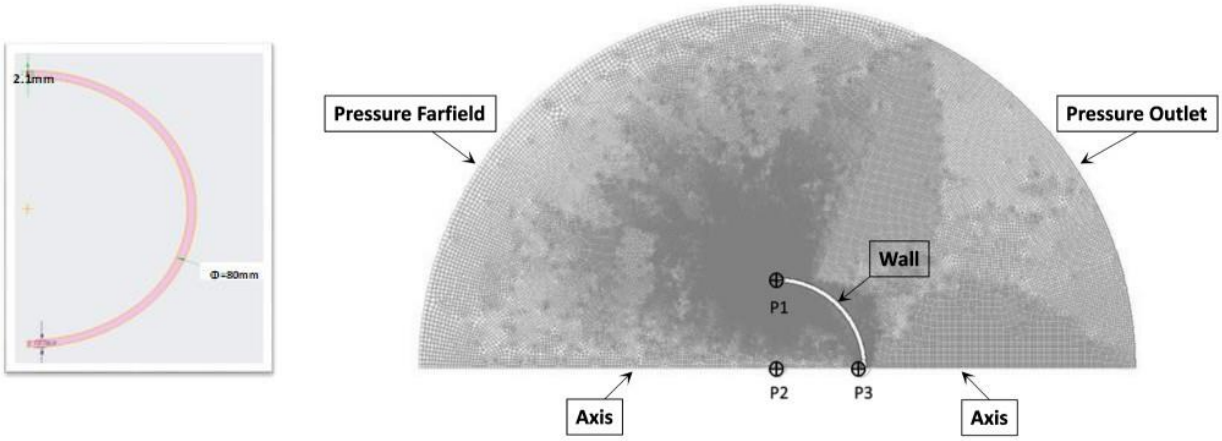


**(a) Geometrical Details** **(b) 2D Computational Domain with Boundary Condition**

**Fig. 1 (a) Geometrical Details, (b) Computational Grid**

Simulation (DES) model is implemented while solving the time resolved flow. To capture unsteady flow field, firstly the steady state solution was achieved using RANS. Further computations were continued using DES with very small time steps ($\Delta t = 10^{-6}$ s) to capture the unsteadiness of flow. Initial unsteady DES computations were made using the 1st order implicit time stepping in order to reduce the flow transition time and then subsequently it was changed to second order for capturing the unsteadiness. Furthermore, the pressure histories at three different locations were monitored to capture and compare the modes of the unsteady flow oscillations over the frontal cavity at different Mach number (Mach 2.00, Mach 4.00 & Mach 6.00). Suitable code validation has been conducted before adopting the above mentioned numerical procedures in the present study. The computational domain, grid generation, boundary conditions adopted for the simulations and solver validation are presented in the next sub-sections.

### C. Computational Domain & Grid Generation

The computational domain consists of a 2D hemispherical concave shell placed within a semi-circular domain as shown in Fig. 2. The domain inlet has been specified with the pressure farfield boundary condition and the domain outlet is specified with the pressure outlet boundary condition. The farfield boundaries are assigned with static pressure and static temperature corresponding to the adopted values of Mach numbers and Reynolds numbers. No slip wall boundary conditions have been enforced on the frontal cavity with suitable near wall treatment for turbulent flows. The boundaries of the computational domain extend from –160 mm to 160 mm in x and 0 mm to 160 mm in y directions with the origin placed at the center of the hemispherical arc. The 1st cell distance near the entire hemispherical cavity is maintained at a distance of 0.005 mm and the total cell count is being used as around 1,80,000 maintaining the wall y+ value on the frontal cavity surface below 5. The appropriate mesh for the present investigation has been selected after conducting suitable grid independence study in [10]. The 2D unstructured grid is generated in computational domain by using the mesh generator in ANSYS Meshing where simulations are carried out on multiple grids of increasing refinement with dividing the domain in such a way that the near wall meshing is very fine to capture the unsteadiness precisely. For the analysis of the Mach number effect on the flow unsteadiness over the frontal cavity, the pressure histories are monitored at three different locations as mentioned in Figure 2. The three different locations lie at the lip corner (Point P1), at the point near the shock formation in front of hemispherical shell (Point P2), and innermost point of hemispherical cavity (Point P3).

### D. Boundary and Initial Conditions

To study the effect of freestream Mach number on the overall flow field, the frontal cavity configuration has been considered and simulated at a flow speed of Mach 2, 4, and 6 with the corresponding freestream Reynolds numbers (based on per meter reference length) of $11.66 \times 10^6$, $22.93 \times 10^6$, and $34.40 \times 10^6$, respectively. The various flow parameters adopted in the present simulations are tabulated in Table 1. The solution approached with a steady state

**Table 1 Flow conditions in test-section [3, 6]**

| Parameter | Values |
|---|---|
| Model Diameter ($D$) | 80.0 mm |
| Shell thickness ($t$) | 2.1 mm |
| Freestream Mach Number ($M_\infty$) | 2, 4 and 6 |
| Stagnation Pressure ($P_0$) | 510 kPa |
| Stagnation Temperature ($T_0$) | 300 K |
| Unit Reynolds Number ($R_e$) (/m) | $11.66 \times 10^6$, $22.93 \times 10^6$ and $34.40 \times 10^6$ |

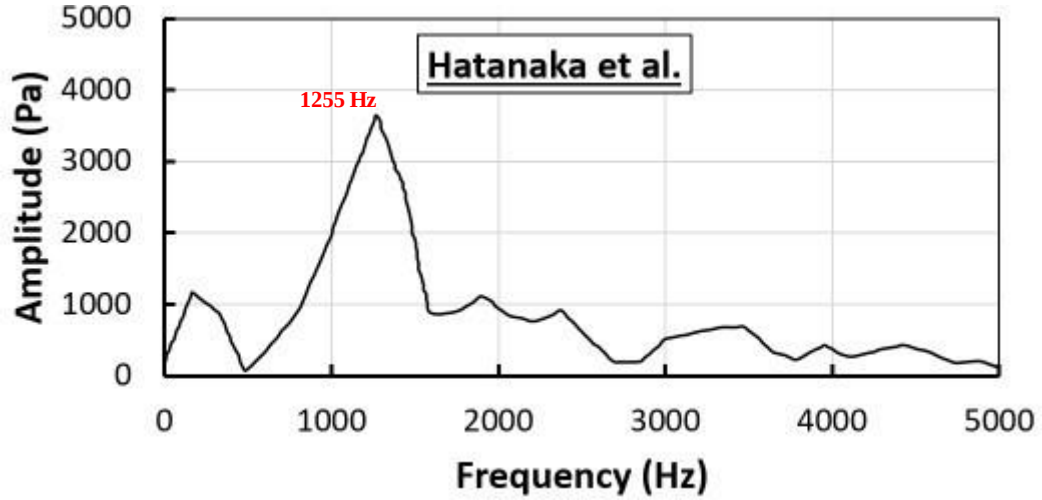


**(a) Experimental Data [3]**

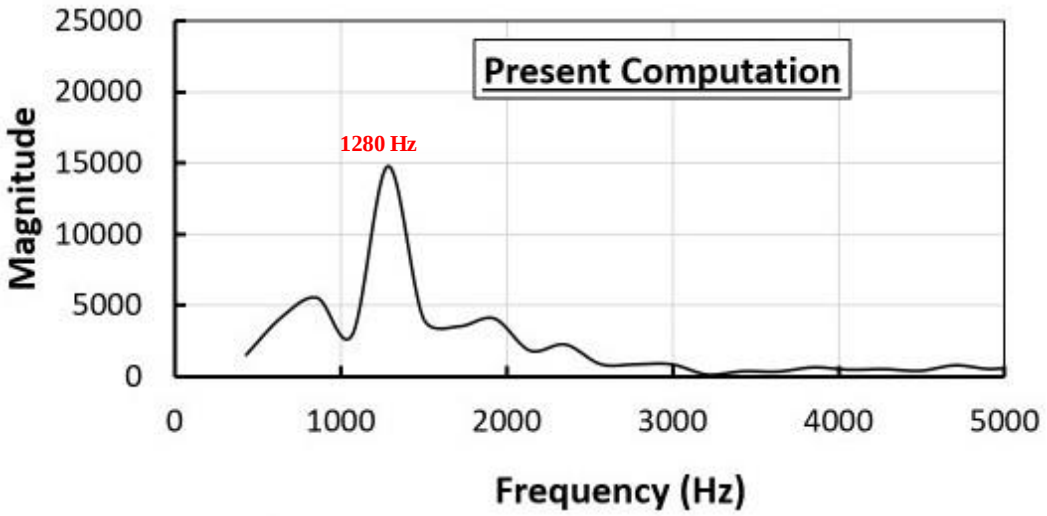


**(b) Present DES Simulations**

**Fig. 2 Comparison between Experimental [3] and Computational Frequency Data (Pressure history at Point 2)**

fed to unsteady simulation which means initially the steady state simulation is performed and once converged, the simulation is switched to transient (DES) phase with a solution time step size of $10^{-6}$ sec. The time step size of $10^{-6}$ sec. has been approached after conducting suitable time-step convergence study [10].

### E. Solver Validation

For the purpose of DES solver validation, DES based time-resolved flow investigation over a frontal cavity model has been carried out as per the geometry and boundary conditions reported in Hatanaka et al. [3, 4]. The computation for the validation of the DES solver has been carried out at a freestream Mach number of 4.0 and Reynolds number of $22.93 \times 10^6$. The pressure history at the center of the frontal cavity (Point-2 as shown in Fig.1) has been monitored and the corresponding frequency spectra has been generated by applying suitable FFT Transformation. The FFT spectra obtained in the present DES Simulation is compared with the FFT spectra reported by Hatanaka et al [3]. The comparison is shown in Fig. 2 and a fair agreement between the reported and the computed spectra can be seen thus validating the DES solver adopted in the present investigation.

## III. Results and Discussions

In the present investigation, 2D axisymmetric DES simulations are performed over the frontal cavity at three different free stream Mach numbers (2.00, 4.00 and 6.00) in order to study the effect of the freestream Mach number on the unsteady flow phenomena on small and large amplitude fluctuations on frontal hemispherical cavity. The simulations performed at Mach 2, 4 and 6 freestream condition in front of concave hemispherical shell are analyzed here by capturing the time history of pressure data collected at three points (Fig. 1) during the whole respective simulations. The previous 3D numerical simulations based on laminar Navier Strokes Equations were unable to capture multiple cycles of large amplitude fluctuations for concave cavity. It was reported [3, 9] that the rapid movement of shock away from the cavity leads to numerical instability in the simulation causing solution breakdown. However, in this study, the DES approach was able to capture the flow fluctuations for multiple cycles. All the computations are performed up to a flow time of 10 ms to capture multiple large amplitude pulsations. In order to perform the comparative study, the pressure history, frequency spectra and the unsteady flow cycles computed over the frontal cavity, for all the three freestream Mach numbers under consideration, are analyzed and are presented in next sub-sections with pressure history plots, frequency plots and Mach contours histories.

### A. Effect of Freestream Mach number on Pressure History

In order to quantitatively analyze the effect of Mach Number on the flow unsteadiness of frontal cavity, the pressure history at three different points have been captured at point P1 (on the lip of the hemispherical cavity), point P2 (center of the cavity) and point P3 (innermost point inside the cavity facing the flow) as shown in Fig. 1. The flow has been analyzed at three different Mach numbers (2.00, 4.00 and 6.00). In the Fig. 3a, 3b, and 3c, which represents the pressure history at point 1, point 2 and point 3 and at different Mach numbers. It can be observed that the most dominating high amplitude pressure oscillations corresponding to the shock pulsations are captured at all the locations, clearly for all the Mach numbers investigated in the present research. Furthermore, with increase in Mach number a significant increase in the amplitude of the pressure fluctuations are observed. From the Fig. 3, it can be observed that Mach 6 shows the highest pressure amplitude whereas Mach 2 shows the minimal pressure amplitude at all three pressure points. In all the cases of Mach numbers (2, 4, & 6) considered in the present study, in addition to the dominant mode, low amplitude sub-dominant modes are also observed to be generated. The amplitude of pressure oscillations for the case of Mach 2.00 is found to be comparatively small and hence the pressure history generated at various points for the case of Mach 2.00 looks to be blunt in the comparison plots in Fig. 3. The peaks at point 1 and 2, reflects the shock movement towards the cavity and seems in phase most of the time, however, there is phase delay between peaks at point 1 and point 3 with sharp peak at point 3. It can be described by high pressure zone inside the cavity and forward motion due to high pressure near the inner most point in hemispherical cavity. The total number of peaks are higher for higher Mach numbers as the fundamental acoustic frequency will increase with increase in Mach number. Although Mach 2 flow shows lower amplitude in comparison to other Mach number, but the frequency of the dominant mode of the flow unsteadiness for Mach 2.00 case can be clearly observed upon FFT transformation and is reported in the subsequent sub-section.

### B. Effect of Freestream Mach number on Frequency Analysis

To understand the effect of the Mach number on various timescale involved in the unsteady flow in front of hemispherical cavity, Fast Fourier Transformation (FFT) of the captured pressure histories at Point 2 at different Mach numbers are obtained. Point 2 is considered more sensitive with respect to small or large amplitude fluctuation of bow shock. Hence, point 2 is selected for frequency analysis. The comparison is shown in Fig. 4. From the FFT comparison, it can be observed that with an increase in Mach number, the frequency of the most dominant mode

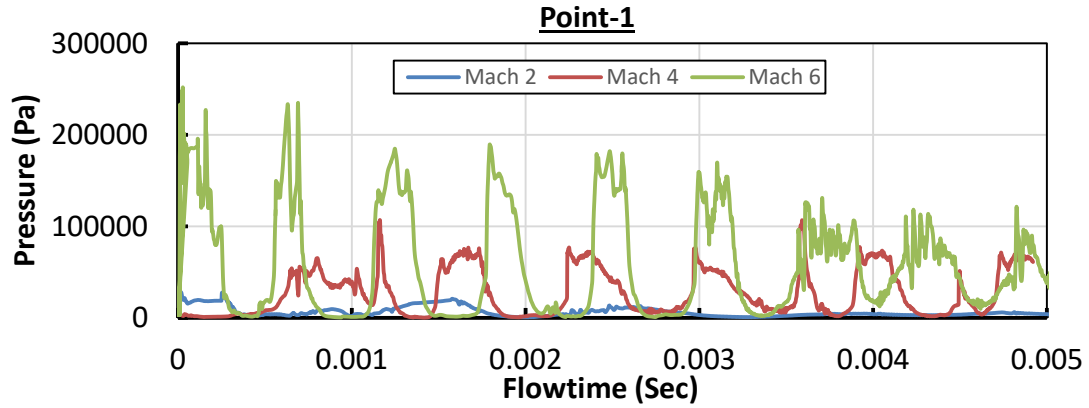


**(a) Pressure History at Point 1**

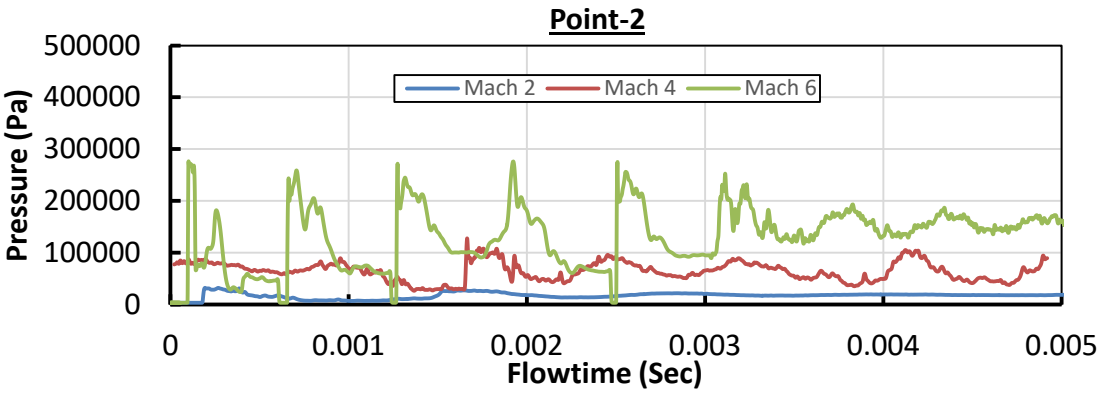


**(b) Pressure History at Point 2**

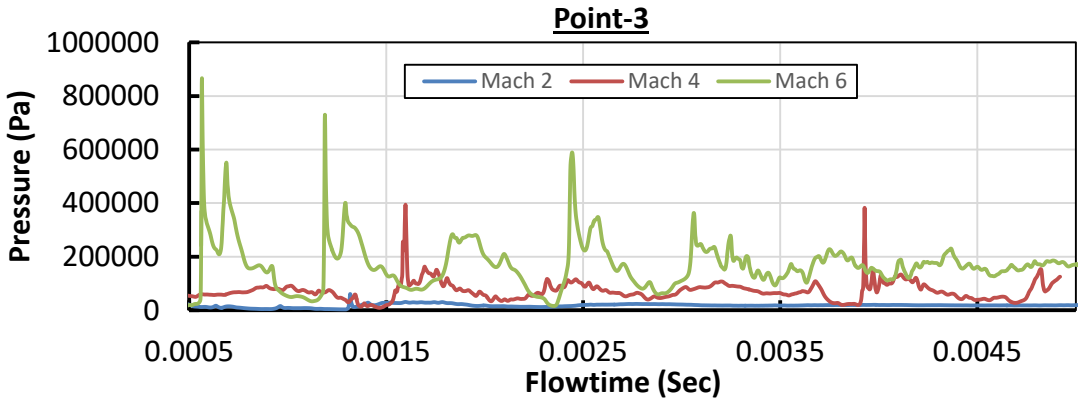


**(c) Pressure History at Point 3**

**Fig. 3 Time history of Static Pressure at three defined points (a) Point P1: Lip corner (b) Point P2: location of bow shock in steady state and (c) Point P3: innermost point in the cavity**

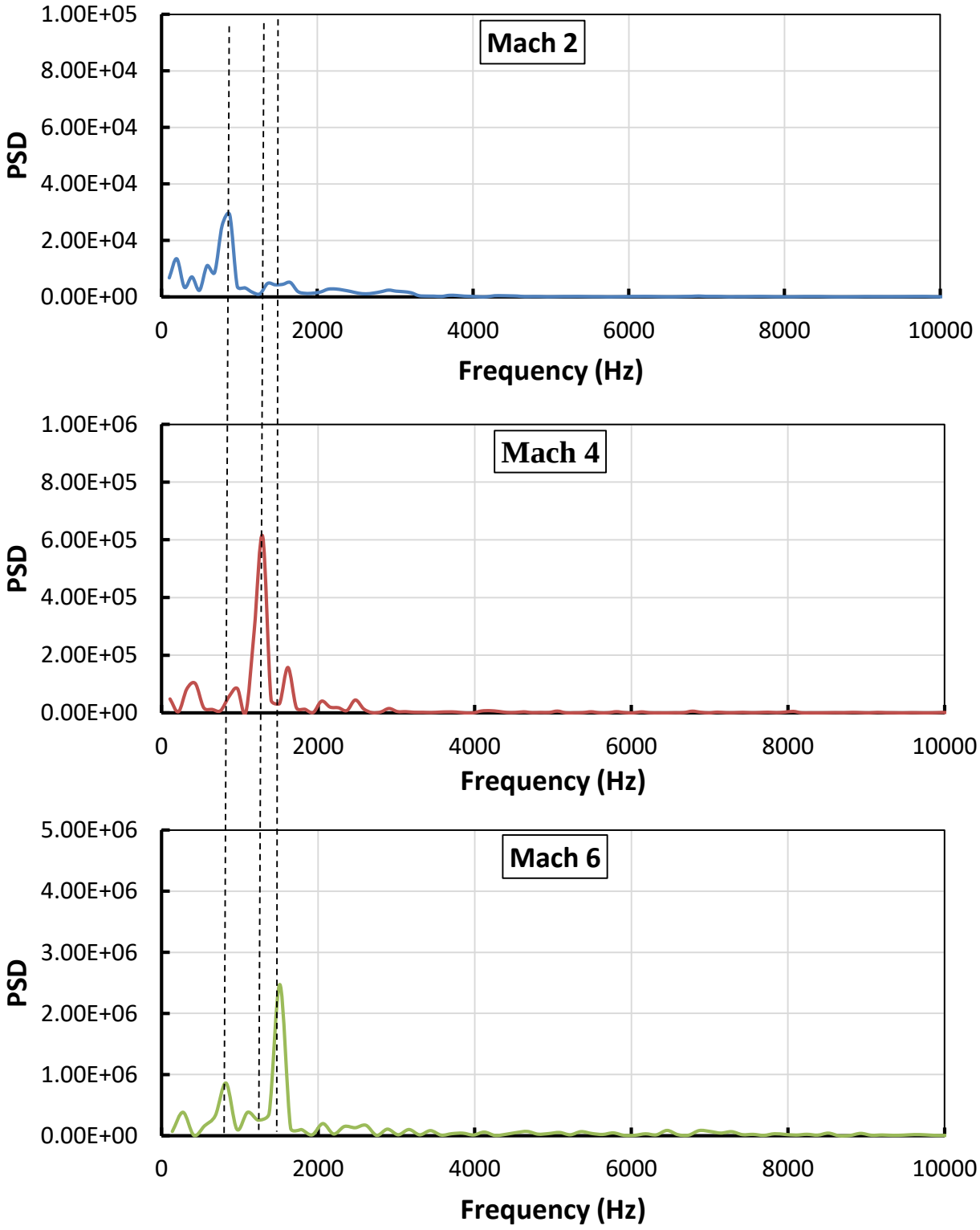


**Fig. 4 PSD plot for pressure data recorded at Point P2: location of bow shock in steady state**

increases significantly. For Mach 2, the frequency of the most dominant mode is found to be 870 Hz. With increase in the free stream flow velocity to Mach 4 the dominant mode is observed to shift to a higher frequency of 1070 Hz. For the case of Mach 6, the frequency was found to be maximum standing at 1510 Hz. As discussed in the previous sub-section, the amplitude of the spectral analysis is also found to be increased with increase in Mach number with Mach 6 generating the maximum amplitude (see Fig. 4c). At Mach 6, in addition to the most dominant mode, a low frequency sub dominant is observed at 824 Hz. Whereas, at Mach 2 additional low amplitude high frequency sub dominant unsteady mode is seen to be generated at around 1500 Hz. However, in the case of Mach 4 additional low amplitude high as well as low frequency sub dominant unsteady modes were observed to be generated at around 1000 Hz and 1500 Hz, respectively. This unique phenomenon needs further in-depth study in future to get a detailed insight in the mechanism behind the generation of such multiple modes.

### C. Effect of Free-stream Mach number on unsteady flow cycle

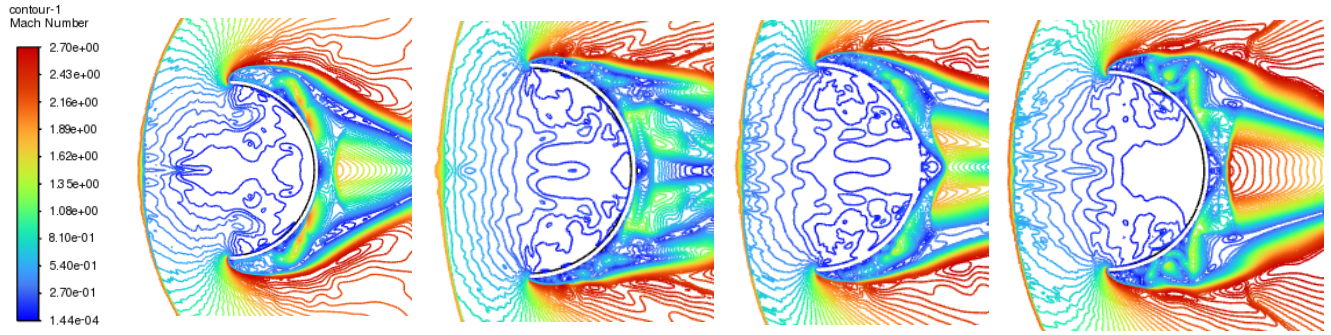


a) Cycle Analysis at Mach 2

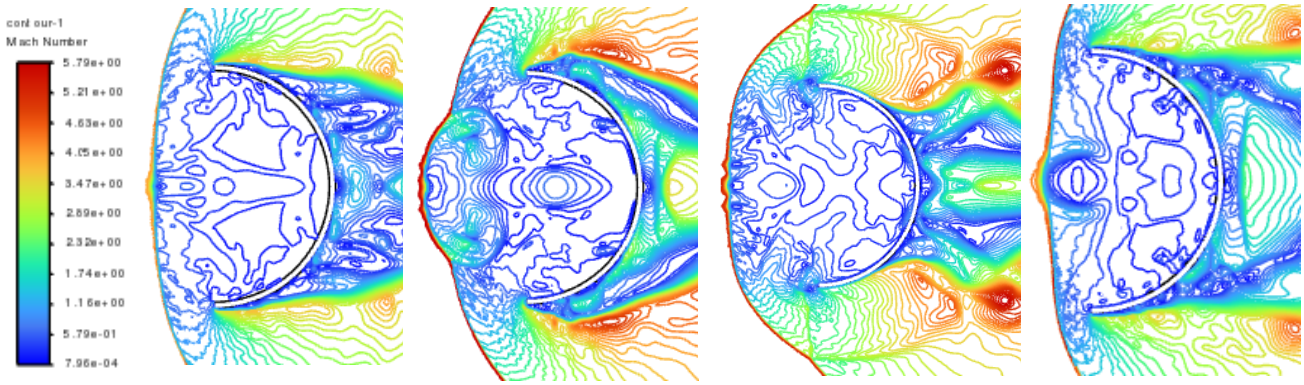


b) Cycle Analysis at Mach 4

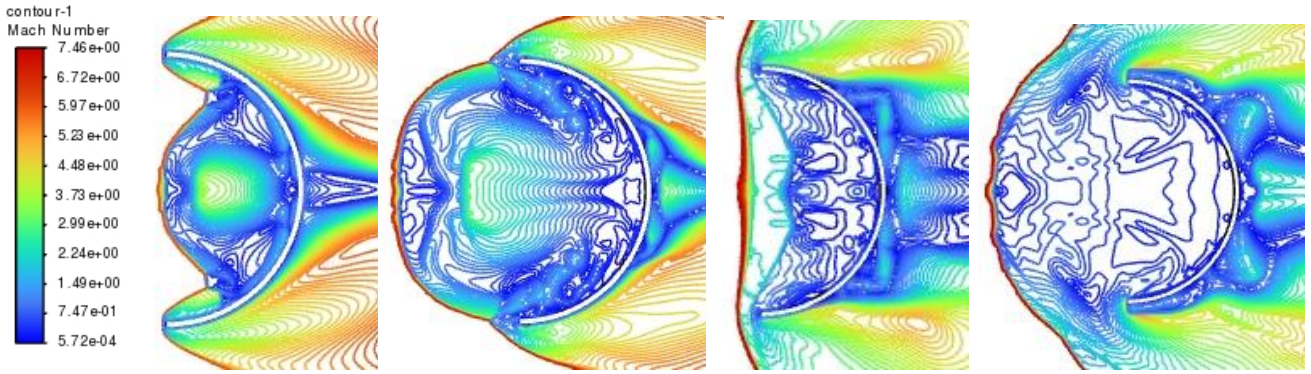


c) Cycle Analysis at Mach 6

**Fig. 5 Flow features through Mach contours at different time stamp (Peak pressure point and Lowest pressure point) during the shock fluctuation cycle (Corresponding to Point-2).**

The flow through Mach contours at different time steps has been captured. As shown in the Fig. 5, a large unsteadiness in the flow can be observed along with the bow shock pulsations at all the different Mach numbers (2, 4 and 6). In addition, for all the cases of freestream Mach numbers under consideration in the present study, the formation of the counter rotating vortices within the shell engulfed cavity region is observed. Along with the vortices, the regions of flow leakage at the cavity corner can be seen to be generating for each of the cases under investigation. These dynamic interaction between vortices and flow leakages plays the major role in driving the pulsating shock wave to and fro the cavity surface with the advancement of the flow time. With an increase in the freestream Mach number, an increase in the shock strength and shock pulsation is observed in the Fig. 5c. As observed in the Fig. 5a at Mach 2 the shock strength is comparatively lower as to that of Mach 4 and at Mach 6 the shock strength is observed to be maximum. Along with the shock strength, there is increase in the spatial extent in the shock pulsation as the Mach number is increased from Mach 2 to Mach 6. These increase in the extent of the shock pulsation there by denotes an increase in the strength of the pulsation and compression due to forward motion of shock, and hence an increase in the amplitude of the flow unsteadiness with increase in the Mach number (as reported in the previous sub-section). However, as the flow speed is increasing along with the increase in the pressure amplitude an increase in the frequency is also observed which is quite expected. Furthermore, with increase in Mach number, along with the change in the amplitude and frequency of the shock oscillation, the formation/emergence of triple point can be observed for the cases of higher freestream Mach number. At Mach 2, the triple point is not seen. However, as the freestream Mach number increases to Mach 4, the triple point is observed, which moves radially outward as time progresses. Finally, the triple point is seen to be diffused into the freestream at the wake of the cavity as seen in the Fig. 5b. On further increasing the freestream Mach number 4 to 6 the triple point is observed to be moving back and forth into and outside the cavity region with the advancing time frame. And, in the case of Mach 6, the triple point is found to reach the closest to the cavity concave surface facing the flow. In addition, the shape of the pulsating bow-shock is also observed to be varying with the increase in Mach number.

## IV. Summary

In this study, the effectiveness of DES simulations to capture the large amplitude bow shock fluctuations at different Mach numbers ranging from supersonic to hypersonic has been demonstrated by using two-dimensional axisymmetric simulation in comparison to previous three-dimensional simulations with significantly lower computation cost. The DES simulation with inclusion of turbulence model captures well the dynamics of vortical structure inside the cavity and its interaction with moving bow shock. The computed frequency of bow shock fluctuations is validated with previous experimental and three-dimensional numerical data. With increase in Mach number, the frequency of main dominant mode increases as well as the amplitude of shock fluctuation increases due to increase in compression within the cavity and strength of bow shock. With the change in freestream Mach number, in addition to the change in the frequency and amplitude of the unsteadiness, a variation in the key flow features such as triple point, shock strength, extent of shock pulsation etc. are also observed.



## References

[1] Xue, X., and Wen, C.-Y., "Review of unsteady aerodynamics of supersonic parachutes," *Progress in Aerospace Sciences*, Vol. 125, 2021, p. 100728. https://doi.org/10.1016/j.paerosci.2021.100728.

[2] Sueki, M., and Mizukaki, T., "Numerical Analysis on Shock waves behavior around aerodynamic decelerator for Mars planetary probe mission," *29th Congress of the International Congress on Aeronautical Sciences*, Russia, 2014.

[3] Hatanaka, K., Rao, S. M. V., Saito, T., and Mizukaki, T., "Numerical investigations on shock oscillations ahead of a hemispherical shell in supersonic flow," *Shock Waves*, 2016, pp. 299–310. https://doi.org/10.1007/s00193-015-0613-0.

[4] Kawamura, T., and Mizukaki, T., "Aerodynamic Vibrations Caused by a Vortex Ahead of Hemisphere in Supersonic Flow," *28th International Symposium on Shock Waves*, edited by K. Kontis, Springer Berlin Heidelberg, Berlin, Heidelberg, 2012, pp. 671–676. https://doi.org/10.1007/978-3-642-25685-1_102.

[5] Vashishtha, A., Watanabe, Y., and Suzuki, K., "Study of Shock Shape in front of Concave, Convex and Flat Arc in Hypersonic Flow," *JAXA-SP-14-010*, 2015, pp. 127–132. URL http://id.nii.ac.jp/1696/00003852/.

[6] Mizukaki, T., and Kawamura, N., "Instability Characteristics of Shock Waves ahead of Hemispherical Shell at Supersonic Speeds," *28th Congress of the International Council of the Aeronautical Sciences*, 2012.

[7] Vashishtha, A., Watanabe, Y., and Suzuki, K., "Study of Bow-Shock Instabilities in front of Hemispherical Shell at Hypersonic Mach Number 7," *45th AIAA Fluid Dynamics Conference*, AIAA 2015-2638, 2015. https://doi.org/10.2514/6.2015-2638.

[8] Vashishtha, A., Watanabe, Y., and Suzuki, K., "Bow-Shock Instability and its Control in front of Hemispherical Concave Shell at Hypersonic Mach Number 7," *Transaction of the JSASS, Aerospace Technology Japan*, Vol. 14, No. ists30, 2016, pp. 121–128. https://doi.org/10.2322/tastj.14.Pe_121.

[9] Vashishtha, A., "Bow-Shock Instability and its Control in front of Concave shaped Blunt Nose at Hypersonic Mach No. 7," Ph.D. thesis, Department of Advanced Energy, 2016. https://doi.org/10.15083/00075323.

[10] Deshmukh, J., Bajaj, D. K., Sahoo, D., and Vashishtha, A., "Unsteady Simulation of Frontal Cavity in Supersonic Flows," *Proceedings of International Conference on Theoretical Applied Computational and Experimental Mechanics, ICTACEM*, 2021.

[11] Hamed, A., Basu, D., and Das, K., *Detached Eddy Simulations of Supersonic Flow over Cavity*, 2017. https://doi.org/10.2514/6. 2003-549